



# Evaluation of the potential of rhTGF- $\beta$ 3 encapsulated P(LLA-CL)/collagen nanofibers for tracheal cartilage regeneration using mesenchymal stems cells derived from Wharton's jelly of human umbilical cord

Jing Wang<sup>a</sup>, Binbin Sun<sup>a</sup>, Lingling Tian<sup>b</sup>, Xiaomin He<sup>c</sup>, Qiang Gao<sup>a</sup>, Tong Wu<sup>a</sup>, Seeram Ramakrishna<sup>b,d</sup>, Jinghao Zheng<sup>c,\*</sup>, Xiumei Mo<sup>a,e,\*\*</sup>

<sup>a</sup> State Key Laboratory of Modification of Chemical Fibers and Polymer Materials, College of Chemistry, Chemical Engineering and Biotechnology, Donghua University, Shanghai 201620, China

<sup>b</sup> Center for Nanofibers and Nanotechnology, E3-05-14, Department of Mechanical Engineering, Faculty of Engineering, National University of Singapore, 2 Engineering Drive 3, Singapore 117576, Singapore

<sup>c</sup> Department of Pediatric Cardiothoracic Surgery, Shanghai Children's Medical Center, Shanghai Jiao Tong University School of Medicine, Shanghai 200127, China

<sup>d</sup> Guangdong-Hongkong-Macau Institute of CNS Regeneration (GHMICR), Jinan University, Guangzhou 510632, China

<sup>e</sup> Shandong International Biotechnology Park Development Co., Ltd., China

## ARTICLE INFO

### Article history:

Received 30 June 2016

Received in revised form 8 September 2016

Accepted 21 September 2016

Available online 21 September 2016

### Keywords:

Nanofibers

rhTGF- $\beta$ 3

Tracheal cartilage regeneration

WMSCs

## ABSTRACT

Tracheal injuries are one of major challenging issues in clinical medicine because of the poor intrinsic ability of tracheal cartilage for repair. Tissue engineering provides an alternative method for the treatment of tracheal defects by generating replacement tracheal structures. In this study, core-shell nanofibrous scaffold was fabricated to encapsulate bovine serum albumin & rhTGF- $\beta$ 3 (recombinant human transforming growth factor- $\beta$ 3) into the core of the nanofibers for tracheal cartilage regeneration. Characterization of the core-shell nanofibrous scaffold was carried out by scanning electron microscope (SEM), transmission electron microscope (TEM), laser scanning confocal microscopy (LSCM), and tensile mechanical test. The rhTGF- $\beta$ 3 released from the scaffolds in a sustained and stable manner for about 2 months. The bioactivity of released rhTGF- $\beta$ 3 was evaluated by its effect on the synthesis of type II collagen (COL2) and glycosaminoglycans (GAGs) by chondrocytes. The results suggested that its bioactivity was retained during release process. The proliferation and morphology analyses of mesenchymal stems cells derived from Wharton's jelly of human umbilical cord (WMSCs) indicated the good biocompatibility of the fabricated nanofibrous scaffold. Meanwhile, the chondrogenic differentiation of WMSCs cultured on core-shell nanofibrous scaffold was evaluated by real-time qPCR and histological staining. The results suggested that the core-shell nanofibrous scaffold with rhTGF- $\beta$ 3 could promote the chondrogenic differentiation ability of WMSCs. Therefore, WMSCs could be a promising seed cells in the construction of tissue-engineered tracheal cartilage. Overall, the core-shell nanofibrous scaffold could be an effective delivery system for rhTGF- $\beta$ 3 and served as a promising tissue engineered scaffold for tracheal cartilage regeneration.

© 2016 Published by Elsevier B.V.

## 1. Introduction

Tracheal defects resulting from diseases such as stenosis, cancer or trauma are becoming a major clinical problem with high mortality rate. Up to now, various options are used to repair tracheal defects, such as direct anastomosis, autografts, allografts and prosthetic materials [1–5]. However, there is no predictably effective treatment that can easily return normal function to the trachea. Therefore, the method

of tracheal tissue engineering using autologous stem cells to generate new tissues has been investigated [6–8]. New tracheal tissues can be created in vitro and then be implanted into the defect area. More importantly, the reconstructed trachea can grow in vivo with the somatic growth of children. Thus, tissue engineering provides a new way for the treatment of tracheal defects by generating replacement tracheal structures. Vacanti et al. firstly reported regeneration of tracheal cartilage using tissue engineering techniques [9].

Although the diversity of the methods for cartilage regeneration via tissue engineering techniques, the three fundamental components routinely required include scaffold, seed cells, and bioactive factors. The scaffolds should have high porosity, good biocompatibility, proper mechanical properties, and appropriate biodegradability [10], which serve as temporary microenvironment to support the cells proliferation and differentiation for regeneration of tissues and organs. Electrospun

\* Correspondence to: J. Zheng, Department of Pediatric Cardiothoracic Surgery, Shanghai Children's Medical Center, Shanghai Jiao Tong University School of Medicine, Shanghai 200127, China.

\*\* Correspondence to: X. Mo, State Key Laboratory of Modification of Chemical Fibers and Polymer Materials, College of Chemistry, Chemical Engineering and Biotechnology, Donghua University, Shanghai 201620, China.

E-mail addresses: [zhengjh210@163.com](mailto:zhengjh210@163.com) (J. Zheng), [xmm@dhu.edu.cn](mailto:xmm@dhu.edu.cn) (X. Mo).

nanofibers which can closely mimic the physical structure of protein fibrils in nanoscale in native ECM could serve as a good tissue engineering scaffold. It is well known that electrospinning is the simplest, least expensive, and quickest technique used to fabricate nanofibers. During electrospinning process, a high voltage is applied to the polymer melt or solution, and the resultant electrical charges will accumulate on the surface of the liquid droplet at the tip of the capillary. Then the Coulombic repulsion of the charges will overcome the surface tension of the polymer droplet at a critical voltage. As a result, a charged jet is ejected from the tip of the droplet. The solvent will be evaporated while the jet travels toward a grounded electrode, and the resultant fibers are collected on a grounded target [11]. Large categories of materials are used to fabricate nanofibers as tissue engineered scaffolds via electrospinning, such as synthetic (PLLA, PCL, P(LLA-CL), PAN) [12–17] and natural polymers (collagen, chitosan, fibrin) [18–20]. In addition to the scaffolds, providing proper seed cells for the regeneration of functional cartilage structures is also a big challenge in tracheal reconstruction. Currently, there is no consensus regarding the ideal cell type for tracheal cartilage regeneration [21]. However, mesenchymal stem cells (MSCs) are a promising seed cell source because of their availability, capacity of expand, and differentiation abilities. Studies have shown the great potentials of MSCs to be able to differentiate toward cartilage in tracheal engineering [21]. Mesenchymal stem cells derived from Wharton's jelly of human umbilical cord (WMSCs) showed a high proliferative rate and were able to differentiate into chondrocytes. It may be a superior source for WMSCs to reconstruct tissue-engineered tracheal cartilage owing to the similar ECM and positive expression of cartilage-specific genes [22].

Apart from being the supporting scaffold structurally, electrospun nanofibers also served as drug delivery system with sustained and controlled release of growth factors/proteins/other drugs functionally. Core-shell structure nanofibers have been extensively used in the controlled delivery of bioactive agents as they can protect its biological activity [23]. The drugs or growth factors do not come into contact with aggressive spinning solvent for the shell materials during the process of electrospinning, avoiding the possibility of being denatured or altered. The recombinant human transforming growth factor- $\beta$ 3 (rhTGF- $\beta$ 3) is a bioactive factor which is essential for chondrogenic differentiation of MSCs in cartilage regeneration [24]. In our study, core-shell structured nanofibers with P(LLA-CL) and collagen as the sheath and bovine serum albumin (BSA)/rhTGF- $\beta$ 3 as the core were fabricated by coaxial electrospinning.

P(LLA-CL) is a US FDA approved synthetic *co*-polymer with nontoxicity, biodegradability, and biocompatibility, which has been investigated in surgery and drug delivery systems [24,25]. However, as the shell of nanofibers, P(LLA-CL) has hydrophobic surface without recognition sites for cell adhesion and spreading. It may prevent the cell-scaffold interactions and the cellular responses. Collagen is a natural polymer material with cell recognition sites which are rich in native cartilage tissues [26]. The combination of these two polymer materials may compensate for the drawbacks of each other and improved the properties of scaffold and enhance the regeneration of tracheal cartilage. The rhTGF- $\beta$ 3 was incorporated into the core of nanofibers with BSA as a protective agent and protein stabilizer.

In this study, we aimed to develop a bioactive nanofibrous scaffold loading rhTGF- $\beta$ 3 via coaxial electrospinning technique, which might promote the chondrogenic differentiation of WMSCs for cartilage regeneration in trachea repair. To further investigate the feasibility of this scaffold, its properties and functions were studied comprehensively.

## 2. Materials and methods

### 2.1. Materials

P(LLA-CL) with a molar ratio of 75% *L*-lactide was purchased from Dai gang Biomaterial Co., Ltd. (Jinan, China). Collagen type I (molecular

weight  $0.8-1 \times 10^5$  Da) was purchased from Ming-rang Bio-Tech Co., Ltd. (Sichuan, China). 1,1,1,3,3,3-Hexafluoro-2-propanol (HFP) was purchased from Co., Ltd. (Shanghai, China). Bovine serum albumin (BSA) was purchased from Sigma-Aldrich (St Louis, MO, USA). Recombinant human TGF- $\beta$ 3 (rhTGF- $\beta$ 3) with molecular weight of 25 kDa and the Elisa kit were purchased from R&D systems (USA). The culture medium and reagents were purchased from Gibco Life Technologies Co. (Carlsbad, California, USA). WMSCs and chondrocytes were provided by Shanghai Children's Medical Center. (Shanghai, China). All chemicals were of analytical grade and were used without further purification.

### 2.2. Fabrication of nanofibrous scaffolds

P(LLA-CL) & collagen were dissolved in HFP with mass ratio of 75/25 at a concentration of 12% and then magnetically stirred at room temperature overnight. The original rhTGF- $\beta$ 3 solution was diluted to  $20 \mu\text{g ml}^{-1}$  with phosphate-buffered saline (PBS) containing 0.1% BSA. Coaxial electrospinning was performed using a common needle electrospinning setup including a high power supply (BGG DC high-voltage generator), and two digitally controlled syringe pumps (KDS200). Apart from this, the special apparatus for coaxial electrospinning is a compound nozzle with an inner needle coaxially placed inside an outer one. The exit orifice diameters of the inner and outer needles were 0.5 and 0.8 mm, respectively. During coaxial electrospinning process, the solution of P(LLA-CL) & collagen and rhTGF- $\beta$ 3 & BSA solution were delivered to the coaxial outer and inner needles, respectively. The applied high voltage and the electrospinning distance were set at 14 kV and 13 cm. The shell solution was injected at a flow rate of  $1.0 \text{ ml h}^{-1}$  and the core solution at  $0.2 \text{ ml h}^{-1}$ . The formed nanofibers were collected by a grounded rotating plate covered with aluminum foil. Then the rhTGF- $\beta$ 3 containing P(LLA-CL)-Collagen nanofibrous scaffold (PC@rhTGF) were obtained by being cross-linked with glutaraldehyde (GTA) vapor formed by 25% GTA aqueous solution for 30 min. The fabricated scaffolds were kept at a vacuum drying oven before further characterization.

The same polymer solution of P(LLA-CL) & collagen used in coaxial electrospinning was also fabricated into blend nanofibers via common electrospinning technique as the control samples. Similarly, the blend P(LLA-CL)-Collagen nanofibrous scaffolds (PC) were obtained by being cross-linked with GTA vapor mentioned above. The resultant scaffolds were kept at a vacuum drying oven before further characterization.

### 2.3. Characterizations of nanofibrous scaffolds

The surface morphologies of the nanofibrous scaffolds were evaluated under a Digital Vacuum Scanning Electron Microscope (SEM, JEOL JSM-5600), Japan) operated at an acceleration voltage of 15 kV. Diameters of fibers were measured with image visualization software Image J (National Institutes of Health, USA) and >100 counts were performed for each scaffold. To verify the core-shell structure of nanofibers, the fibers were collected on carbon-coated Cu grids and observed by transmission electron microscope (TEM, Hitachi H-800, Japan). Fluorescein isothiocyanate conjugated BSA (FITC-BSA) was used as the stabilizer instead of BSA to evaluate the distribution of rhTGF- $\beta$ 3 in the core of nanofibers by laser scanning confocal microscopy (LSCM).

The mechanical properties of nanofibrous scaffolds were performed by a universal materials tester (H5K-S, Hounsfield, UK) at an ambient temperature of  $20^\circ\text{C}$  and humidity of 65%. The size of samples for this test was  $30 \times 10 \text{ mm}$ . A cross-head speed of  $10 \text{ mm min}^{-1}$  was applied for all specimens during the process.

### 2.4. The encapsulation efficiency of rhTGF- $\beta$ 3 in PC@rhTGF nanofibrous scaffold

About 50 mg of PC@rhTGF nanofibrous scaffold was dissolved in 4 ml dichloromethane/PBS solution. The P(LLA-CL) of the scaffold was

dissolved in dichloromethane, while the collagen, rhTGF- $\beta$ 3 and BSA were dissolved in PBS. Further, the mixed solution was centrifuged at 4000 rpm for 5 min. Then, aqueous supernatant was removed to determine the concentration of rhTGF- $\beta$ 3 by Elisa kit according to the manufacturer's protocol. The encapsulation efficiency (EE%) was calculated according to the following equation:  $EE\% = M_1/M_0 \times 100\%$ , where  $M_1$  is the actual amount of rhTGF- $\beta$ 3 measured by Elisa kit and  $M_0$  is the total amount of rhTGF- $\beta$ 3 in 50 mg PC@rhTGF nanofibrous scaffold theoretically.

### 2.5. The release profile of rhTGF- $\beta$ 3 and degradation of PC@rhTGF nanofibrous scaffold in vitro

To determine the in vitro release profile of rhTGF- $\beta$ 3 from PC@rhTGF nanofibrous scaffold, a weighed amount (50 mg) of the scaffold was immersed in 5 ml PBS solution at pH 7.4. Samples were placed in a shaking incubator (150 rpm) at 37 °C. At each time point, 2 ml of release solution was collected from each sample, and replaced by an equal volume of fresh PBS. The concentration of rhTGF- $\beta$ 3 in collected release solution was measured using the rhTGF- $\beta$ 3 Elisa kit according to the manufacturer's protocol. The released profile was calculated as the mass percentage of actual amount for encapsulation over time. The experiments were conducted in triplicate.

In order to study the degradation of PC@rhTGF nanofibrous scaffolds, the morphology changes of the scaffolds were observed after different degradation time. In detail, the scaffolds were taken out from the PBS solution and freeze dried after immersing for 1, 2, 3 months in shaking incubator (150 rpm) at 37 °C. The morphology of the dried scaffolds was observed by SEM. The PC nanofibrous scaffolds were used as control.

### 2.6. The bioactivity of released rhTGF- $\beta$ 3

Previously studies have shown that the synthesis of collagen type II (COL2) and glycosaminoglycans (GAGs) by chondrocytes can be enhanced by rhTGF- $\beta$ 3 [27]. Thus, the bioactivity of rhTGF- $\beta$ 3 released from the scaffolds was analyzed by evaluating its effect on the synthesis of COL2 and GAG by chondrocyte. In brief, the rat chondrocytes were cultured in Dulbecco's modified Eagle's medium (DMEM) in cell culture flasks. When the confluence was about 90%, the cells were trypsinized and seed into 24-well plates. After culturing for 1 day, the cells were divided into two groups: Group I was cultured only with DMEM; Group II was cultured with DMEM supplemented with the released solution of rhTGF- $\beta$ 3 (released for 8 weeks). Both of the two groups were cultured for 14 days and 21 days. At this two time points, the COL2 and GAGs synthesized by chondrocytes were analyzed by immunofluorescence and histological staining, respectively.

### 2.7. The proliferation and morphology of WMSCs on nanofibrous scaffolds

WMSCs were cultured in low glucose DMEM with 10% fetal bovine serum (FBS) and 1% antibiotics in cell culture flasks. The cells were cultured until 90% confluence, and then they were observed by optical microscope (OM) and identified by flow cytometer (FCM). For cell seeding nanofibrous scaffolds were sterilized under the alcohol steam for 3 h and washed with PBS 3 times. The WMSCs were seeded on to round nanofibrous scaffolds (15 mm in diameter) and tissue culture polystyrene (TCP) as a control group in 24 well plates at a density of  $10^4$  cells  $\text{cm}^{-2}$ .

Good biocompatibility is required for tissue-engineered scaffold. The biocompatibility of tissue-engineered includes the ability to perform as a substrate which can support the appropriate cellular activity such as cell adhesion, proliferation, migration and differentiation in order to facilitate tissue regeneration. A desired tissue-engineered scaffold should not elicit any undesirable effects in those cells, or induce any undesirable local or systemic responses in the eventual host. Thus good

biocompatibility is critical for the biomaterials used for tissue engineering [28]. In order to investigate the biocompatibility of the fabricated nanofibrous scaffold, the proliferation of MSCs on scaffolds and TCP was measured by MTT assay which was conducted after culturing for 1, 4, 7 days. Briefly, the cells on scaffolds and TCP were incubated with 360  $\mu$ l pure DMEM and 40  $\mu$ l 5 mg  $\text{ml}^{-1}$  3-(4,5-dimethyl-2-thiazolyl)-2,5-diphenyl-2H-tetrazolium bromide (MTT) for 4 h in incubator at 37 °C. After that, the DMEM was removed and 500  $\mu$ l dimethylsulfoxide (DMSO) was added. To dissolve the formed blue-purple crystal completely, the plate should be incubated in a shaker at 37 °C for 30 min. Subsequently, 100  $\mu$ l of the solution was pipetted in to 96-well plate and measured the absorbance by a microplate reader (Multiskan MK3, Thermo, USA) under 492 nm.

To observe the cells morphology, WMSCs on scaffolds were fixed with 4% paraformaldehyde for 30 min at 4 °C after culturing for 7, 14 days. Thereafter, the scaffolds with cells were dehydrated with gradient ethanol and dried under blowing overnight. Then, the samples were sputter-coated with gold and observed under SEM.

### 2.8. The chondrogenic differentiation of WMSCs on nanofibrous scaffolds

To detect the chondrogenic differentiation of WMSCs cultured on different scaffolds, the gene expression of hyaline cartilage-specific markers such as Sox9 and COL2 were examined using real time-qPCR (RT-PCR) after culturing 14 days and 21 days. Briefly, the cells were fixed with 4% paraformaldehyde for 30 min at 4 °C. Then the RNA was isolated and converted to cDNA using reverse transcriptase (Applied Systems, Foster City, CA, USA). Real-time polymerase chain reaction (PCR) was performed on an Applied Biosystems 7300 (Applied Systems, Foster City, CA, USA) using Taqman primers and probes specific for glyceraldehyde-3-phosphate dehydrogenase (GAPDH) and other relative genes. Sequences of the primers used are listed in Table 1. The relative gene expression was calculated using the  $2^{-\Delta\Delta C_t}$  method with GAPDH as the reference gene.

To detect the GAGs secreted by WMSCs on different scaffolds, histological staining was performed. After culturing for 21 days, cell-scaffold constructs were fixed with 4% paraformaldehyde for 30 min at 4 °C, embedded in paraffin and then sectioned into 5  $\mu$ m section. The sections were stained with Toluidine blue and Safranin O to locate the GAGs deposits.

### 2.9. Statistical analysis

All the data were obtained at least in triplicate and the values were expressed as means  $\pm$  standard deviation (SD). Statistical analyses were performed by the one-way analysis of variance (one-way ANOVA) using Origin 8.5 (OriginLab Inc., USA). The statistical difference was considered statistically significant at  $P < 0.05$ .

## 3. Results and discussion

### 3.1. Characterizations of nanofibrous scaffolds

Nanofibers which can closely mimic the physical structure of protein fibrils in nanoscale in native ECM could serve as a good tissue engineering scaffold. PC@rhTGF and PC nanofibrous scaffold were fabricated by coaxial electrospinning and simple electrospinning technique. As collagen is hydrosoluble, GTA vapor crosslinking was used to prevent the

**Table 1**  
Sequence of primers used for RT-PCR.

Gene	Forward primer	Reverse primer
GAPDH	5'-TGGCGCTGAGTACGTCGTG-3'	5'-ATGGCATGGACTGTGGTCAT-3'
Sox9	5'-CCCTCAACCTCCCACTAC-3'	5'-TCCTCAAGGTCGAGTGAGCTG-3'
COL2	5'-ACGGCGGCTCCACTTCAGC-3'	5'-TTGCCGGCTGCTTCGTCAG-3'

collagen from being dissolved in water. The morphology of the fabricated PC@rhTGF and PC nanofibrous scaffolds were observed by SEM, which is shown in Fig. 1. The nanofibers were uniform, smooth, and bead free, with interconnected pores. The average fiber diameter of PC@rhTGF nanofibrous scaffold was  $502.92 \pm 176.90$  nm, while the value of PC nanofibrous scaffold was  $295.71 \pm 70.63$  nm, indicating of an increased fiber diameter with the encapsulation of BSA & rhTGF- $\beta$ 3.

The core-shell structure of single fibers were studied by TEM and LSCM. The green fluorescent light coming from the FITC-BSA indicated the distribution of proteins in the nanofibers (Fig. 2a), which confirmed the successful incorporation of BSA & rhTGF- $\beta$ 3 in the fibers. Fig. 2b showed the core-shell structure of nanofiber with P(LLA-CL) & collagen in the shell and BSA & rhTGF- $\beta$ 3 in the core. The core-shell structure was uniform and the proteins were distributed in the core of the nanofibers homogeneously.

The first successful human tracheal transplantation was conducted by using decellularized tissues with stem cells [6], unfortunately followed by the failure of functional recovery of trachea due to the collapse of graft after the transplantation, indicating the essential role of mechanical property for bioengineered trachea. The cartilage portion of trachea covers about 2/3 of the circumference providing the structural support while the remaining 1/3 is composed of smooth muscles [21]. The flexibility and stiffness of the cartilage in the reconstructed tracheal tissues is a crucial factor in preventing the collapse problem. The mechanical properties are very important for the success of tissue repair. The mechanical properties of nanofibrous scaffolds were characterized by tensile measurement, which were shown in Fig. 2c. As shown by the curve, the breakage style of both scaffolds experienced two stages during stretch. Firstly, it showed a linear elastic behavior with a higher initial modulus due to the cross-linked collagen in the scaffolds. Then it turned into a stable stage with slower increased tensile strength until the final fracture due to the P(LLA-CL) in the scaffolds. It can be seen that the both the tensile strength and elongation at a break were decreased with the incorporation of BSA & rhTGF- $\beta$ 3. The tensile strength of the nanofibrous scaffolds at a break decreased from  $9.01 \pm 0.54$  MPa to  $6.09 \pm 0.27$  MPa. As for the elongation, the value dropped from  $36.87 \pm 1.35\%$  to  $21.25 \pm 2.97\%$ . The Young's modulus of PC and PC@rhTGF nanofibrous scaffolds were  $106.08 \pm 18.51$  MPa and  $109.20 \pm 15.36$  MPa, respectively. So the Young's modulus of the scaffold changed little after the encapsulation of BSA & rhTGF- $\beta$ 3. This results may be attributed to the BSA & rhTGF- $\beta$ 3 in the core of the nanofibers which

contributed much less to the mechanical performance due to that both were proteins with low molecular weights. As reported, the equilibrium tensile modulus of human tracheal cartilage was found to decrease with depth; from  $13.6 \pm 1.5$  MPa for the abluminal superficial zone to  $4.6 \pm 1.7$  MPa in the middle zone [29]. The mechanical properties of PC@rhTGF nanofibrous scaffolds were able to match that of native tracheal cartilage.

### 3.2. The in vitro release profile of rhTGF- $\beta$ 3 and the degradation of PC@rhTGF nanofibrous scaffold

The encapsulation efficiency was evaluated according to the method aforementioned, and the EE% for PC@rhTGF nanofibrous scaffold was  $45.0 \pm 6.5\%$ . Parts of rhTGF- $\beta$ 3 was lost during the process of electrospinning and cross-linking. Non-uniform fibers may form during the coaxial electrospinning [30], and the proteins may be distributed on the surface of the fibers instead of within the core [31]. In addition, some rhTGF- $\beta$ 3 may lost biological activity during the process of cross-linking with GTA vapor.

The rhTGF- $\beta$ 3 released from PC@rhTGF nanofibrous scaffold was shown in Fig. 3a. The cumulative release of rhTGF- $\beta$ 3 was observed for 57 days with a release rate of up to 82.7%. As mentioned above, some of the rhTGF- $\beta$ 3 appearing on the surface resulted in an initial burst release (about 15%) followed by a relatively slow release. After 57 days, the amount of rhTGF- $\beta$ 3 released from PC@rhTGF nanofibrous scaffold reached 82.7%. Previous studies have shown that the release behavior of proteins encapsulated in the core of coaxial nanofibers is generally affected by the hydrophilicity, degradation, defects of shell part and the co-encapsulation of stabilizer such as BSA [32–35]. In this study, the degradation of P(LLA-CL) & collagen, the uniform of core-shell structure of nanofibers, and the BSA may together contribute to the sustained & stable released behavior of rhTGF- $\beta$ 3.

Fig. 3b showed the SEM images of PC and PC@rhTGF nanofibrous scaffolds with different degradation time. Generally, more obvious morphology changes were presented in PC@rhTGF nanofibrous scaffold compared with PC nanofibrous scaffold for a degradation of 2 months, which was attributed to the release of BSA & rhTGF- $\beta$ 3. Higher level of swelling was observed for the nanofibers of PC@rhTGF scaffold. Conversely, the degradation of scaffold also affected the release profile of rhTGF- $\beta$ 3 from the scaffold. After 3 months, the fibrous structure of PC@rhTGF became more blurred than that of PC. The core-shell

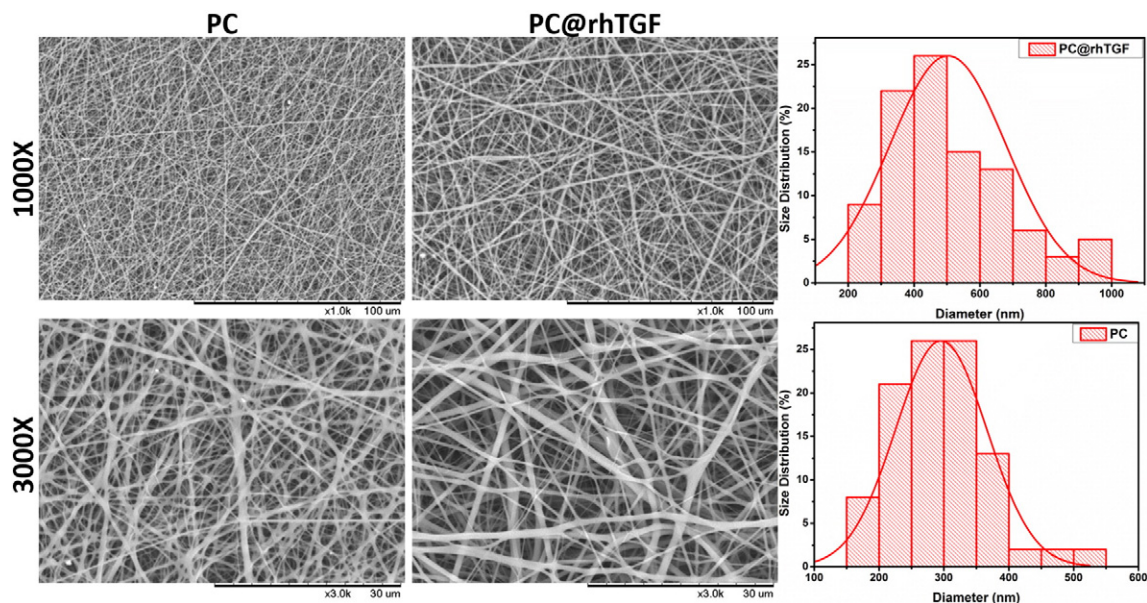
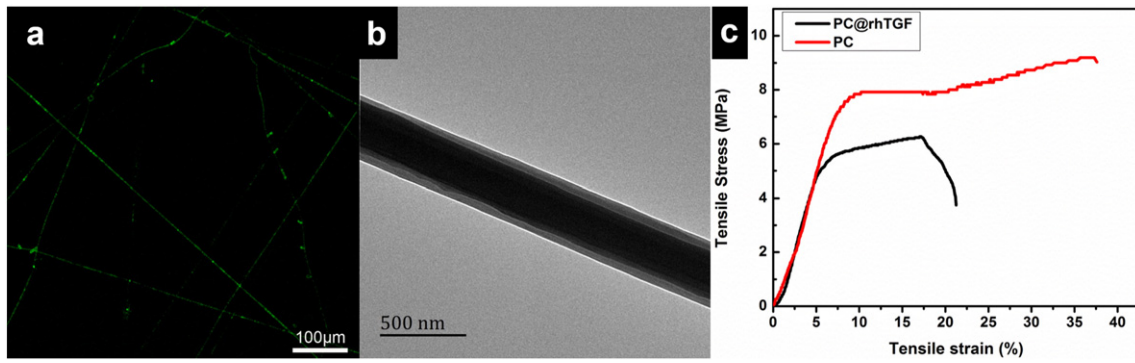


Fig. 1. SEM images of PC@rhTGF and PC nanofibrous scaffolds as well as the distribution of their diameters.



**Fig. 2.** (a) Fluorescence microscopic image of PC@rhTGF nanofibrous scaffold with FITC-BSA & rhTGF-β3 in the core. (b) TEM micrograph of PC@rhTGF nanofiber. (c) Stress-strain curves of PC and PC@rhTGF nanofibrous scaffolds.

nanofibers became hollow with release of the proteins, which resulted in the curly, collapsed and rough appearance for the nanofibers. With the scaffold degradation and proteins release, eroded-like surface morphology and indistinct fiber structure were observed. Swelling of nanofibers were also observed for post-release fibers.

3.3. The bioactivity of released rhTGF-β3

The bioactivity of released rhTGF-β3 was determined by its effect on the synthesis of COL2 and GAGs by chondrocytes. Immunofluorescence staining was conducted to determine the COL2 synthesized by chondrocytes after culturing 14 days and 21 days respectively. As shown in Fig. 4, compared to chondrocytes cultured in normal medium (Group II), more COL2 was synthesized by chondrocytes cultured in medium supplemented with rhTGF-β3 release solution (Group I). The GAGs expressed by chondrocytes was evaluated by histological staining

with toluidine blue and safranin O (Fig.5). Similarly, there was more GAGs synthesized by chondrocytes cultured with medium containing rhTGF-β3 release solution (Group I). The released rhTGF-β3 promoted the COL2 and GAGs expression of chondrocytes, which indicated the bioactivity of rhTGF-β3 released from PC@rhTGF nanofibrous scaffold. This could be attribute to the advantage of coaxial electrospinning, as the shell part of nanofibers could protect the proteins within the core [36]. BSA was used as a protective agent and protein stabilizer for bioactive factors, which also helped in preserving the bioactivity of rhTGF-β3 [33,37].

3.4. The proliferation and morphology of WMSCs on nanofibrous scaffolds

The ideal tissue engineered scaffold should be designed to have excellent biocompatibility to promoting cell proliferation and growth [38]. Before the proliferation study, the WMSCs were observed by OM

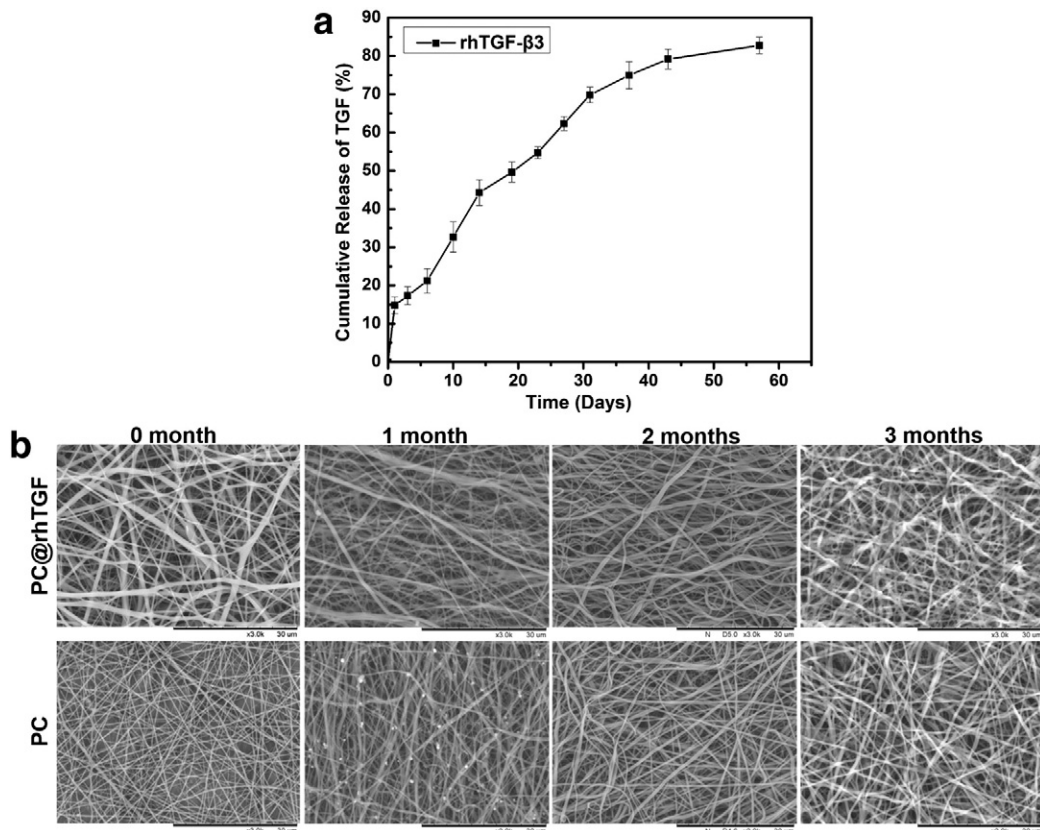


**Fig. 3.** (a) Release profile of rhTGF-β3 from PC@rhTGF nanofibrous scaffold. (b) SEM images of PC@rhTGF and PC nanofibrous scaffolds before and during degradation process.

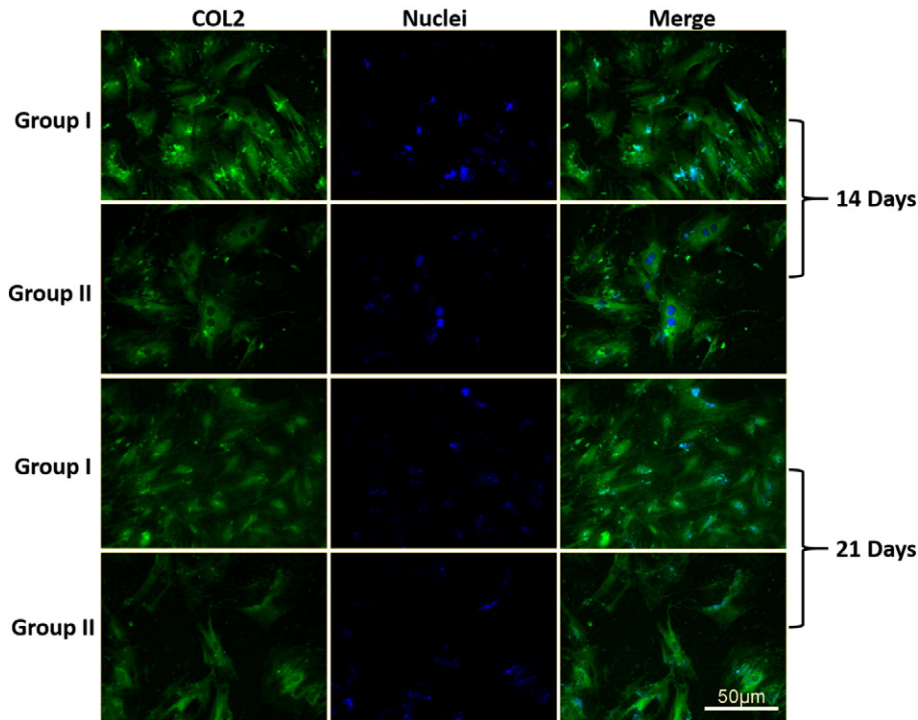


**Fig. 4.** Immunofluorescence staining of COL2 synthesized by chondrocytes cultured with different medium for 14 and 21 days. Group I: cultured with DMEM supplemented with released solution of rhTGF- $\beta$ 3; Group II: cultured with common DMEM. Green: COL 2; Blue: nucleus.

and identified by FCM. Fig. 6a showed that the WMSCs at 4 passage showed a homogenously spindle-shaped cellular morphology. Fig. 6b showed the flow cytometric analysis of surface-marker expression on WMSCs. The phenotypes of WMSCs were negative for hematopoietic-related cell antigens, such as CD34 and CD45. On the contrary, they showed high expression of mesenchymal progenitor cell-related

antigens, such as CD13, CD44, CD73 and CD90. The results showed that the cells isolated from Wharton's jelly only include mesenchymal stem cells. As shown in Fig. 7a, the cells proliferated faster in both nanofibrous scaffolds than in TCP, which indicated the good biocompatibility of nanofibrous scaffolds toward promoting the proliferation of WMSCs. Both P(LLA-CL) and collagen are widely used biomaterials

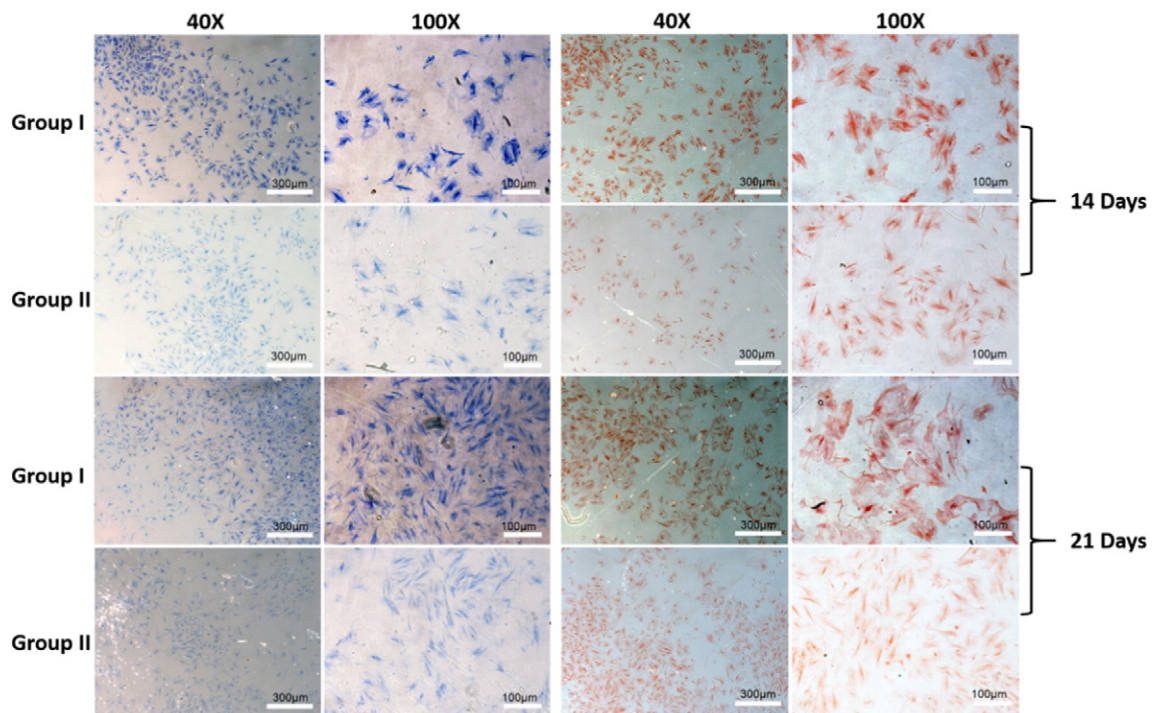


**Fig. 5.** Histological staining of GAGs synthesized by chondrocytes cultured with different medium for 14 and 21 days. Group I: cultured with DMEM supplemented with released solution of rhTGF- $\beta$ 3; Group II: cultured with common DMEM. Blue: Toluidine blue; Red: Safranin O.

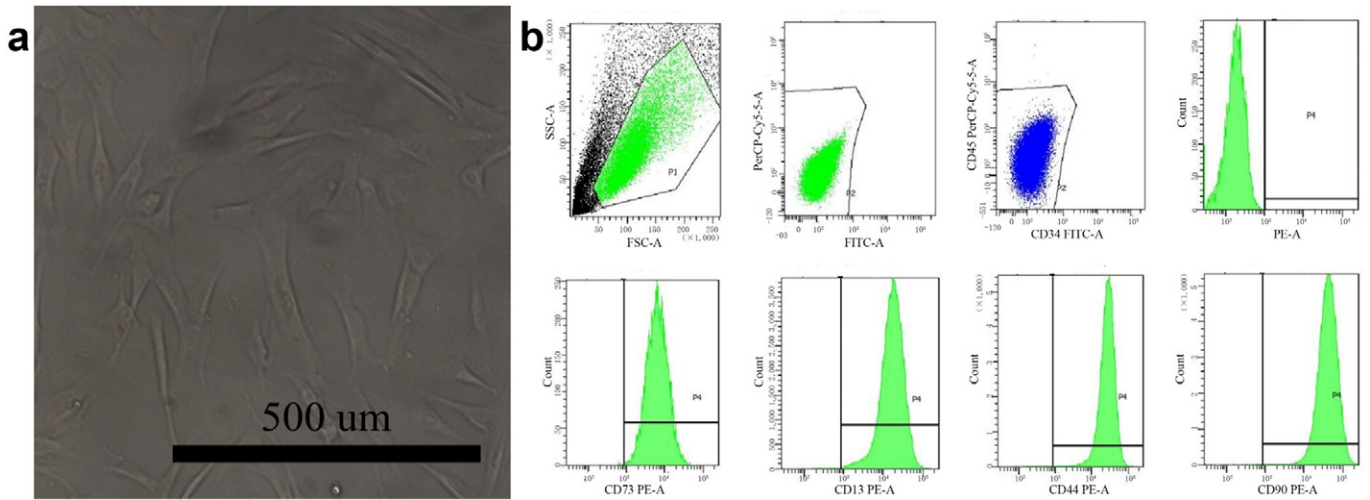


**Fig. 6.** (a) Morphology of WMSCs at 4 passage observed by OM. (b) Flow cytometric analysis of surface-marker expression on WMSCs. Positive expression of CD13, CD44, CD73, CD90 and negative expression of CD34, CD45.

with good cytocompatibility for tissue engineering. Nanofibers with the similar structure to native ECM could also benefit to the cells growth [39,40]. The cells on PC@rhTGF nanofibrous scaffolds showed slower proliferation, which indicated the released rhTGF-β3 from the PC@rhTGF inhibited the proliferation of WMSCs. Because the biological function of rhTGF-β3 is to induce the differentiation of stem cells into chondrocytes, which was evaluated in the following study.

In addition to the proliferation, the morphology of WMSCs on both PC and PC@rhTGF nanofibrous scaffolds were observed by SEM. As shown in Fig. 7b, the nanofibrous scaffolds were able to provide an excellent microenvironment with interconnected pores for cells growth. The cells showed good spreading behavior, especially on PC@rhTGF nanofibrous scaffold. After culturing for 21 days, the cells were well integrated with the nanofibers. The large surface area of nanofibers provide enough space for cell migration and spreading.

3.5. The chondrogenic differentiation of WMSCs cultured on scaffolds

The PC@rhTGF nanofibrous scaffold was further evaluated for its ability to promote WMSCs chondrogenic differentiation, with PC nanofibrous scaffold as control. The expression of the chondrogenic markers Sox-9 and COL2 in WMSCs was determined by RT-PCR. The level of expression of each target gene was normalized to GAPDH. Fig. 8a showed that more cartilage-specific genes expressed on PC@rhTGF nanofibrous scaffolds than the PC nanofibrous scaffolds after 2 weeks

incubation. This could be due to the absence of rhTGF-β3 in PC nanofibrous scaffold.

The GAGs is one of the main component of the ECM in native cartilage. In order to further determine the chondrogenic differentiation of WMSCs, the histological staining was used to locate the GAGs synthesized by WMSCs. The results of Toluidine blue and Safranin O staining of GAGs were shown in Fig. 8b. Toluidine blue and Safranin O positive staining indicated the distribution of GAGs within the nanofibrous scaffolds. It showed that there was more GAGs synthesized by WMSCs on PC@rhTGF nanofibrous scaffolds than that on PC nanofibrous scaffolds. All these data indicated that the rhTGF-β3 released from PC@rhTGF nanofibrous scaffolds in a sustained manner could promote the chondrogenic differentiation of WMSCs. Many studies have shown that encapsulation of drug or protein in the core of the core-shell nanofiber resulted in release profile following a slow and steadily increasing pattern; In contrast, an initial burst release occurs at the beginning of the release process for drug or protein within the blended nanofiber. [41–43]. Additionally, the entire release process of drug or protein within blended nanofibers only lasts for a short time. The long lasting and steadily increasing release of rhTGF-β3 from core-shell PC@rhTGF nanofibrous scaffold affected the differentiation behavior of MSCs in term of providing continuous and bioactive rhTGF-β3 which plays an important role in chondrogenic differentiation of MSCs. According to the release profile of rhTGF-β3, the cumulative release amount after 14 and 21 days could lead to more cell differentiation on PC@rhTGF nanofibrous scaffold compared to the cell differentiation on PC

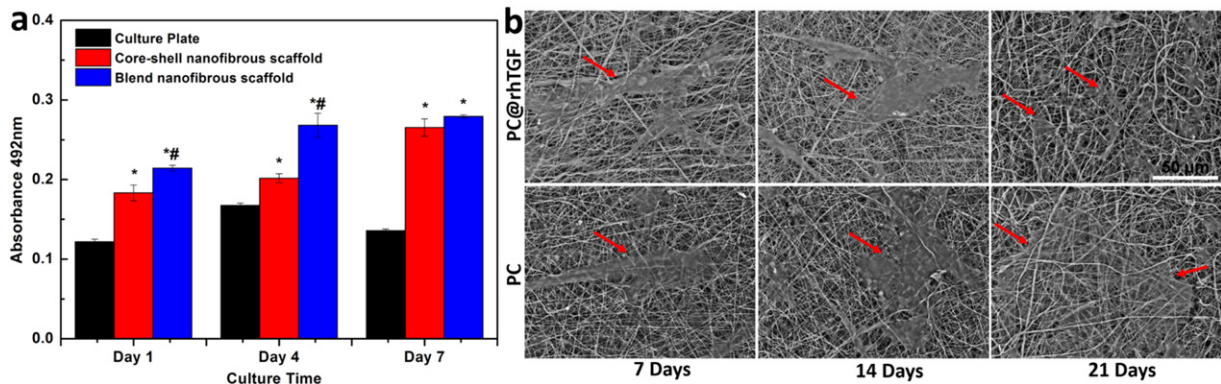


**Fig. 7.** (a) Proliferation of WMSCs on TCP and two different nanofibrous scaffolds in 7 days. \* indicates statistically difference compared to culture plate group ( $P < 0.05$ ); # indicates statistically difference between PC and PC@rhTGF nanofibrous scaffolds groups ( $P < 0.05$ ). (b) SEM images of WMSCs cultured on two different nanofibrous scaffolds for 7, 14, and 21 days.

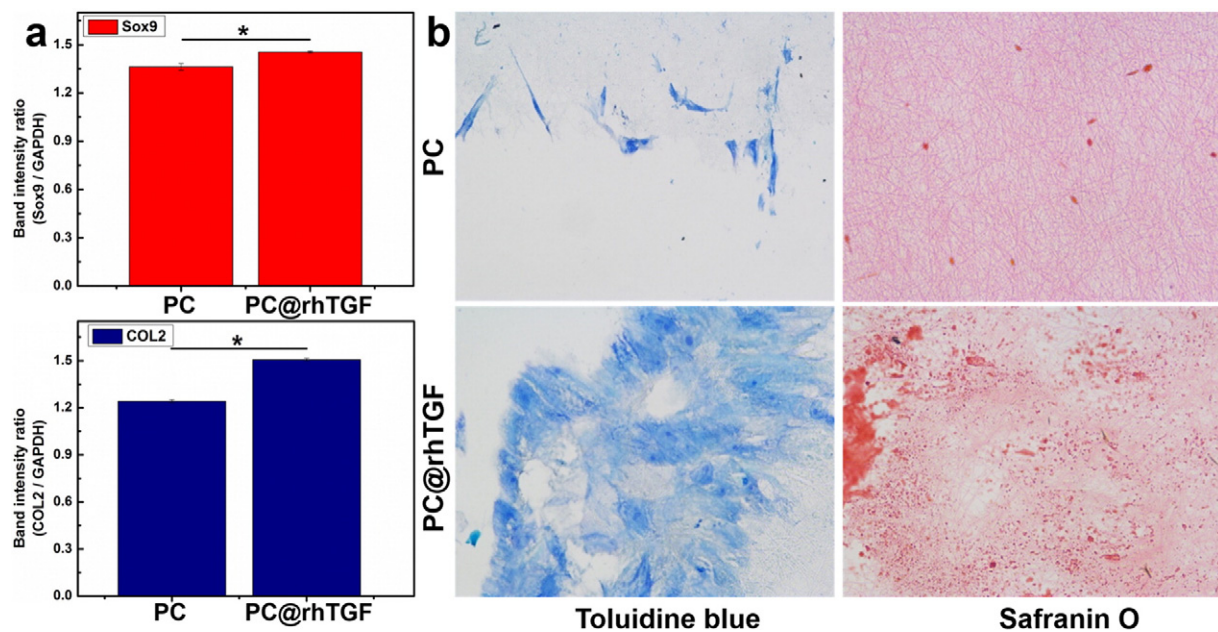


**Fig. 8.** Analyses of chondrogenic differentiation for WMSCs on two different nanofibrous scaffolds. (a) RT-PCR analysis of Sox9 and COL2 gene expression of WMSCs after culturing 14 days. ( $n = 3$ , \* $P < 0.05$ ). (b) Histological staining of GAGs synthesized by WMSCs with Toluidine and Safranin O after culturing 21 days.

nanofibrous scaffold. Thus, the PC@rhTGF nanofibrous scaffold could be a good delivery system for rhTGF- $\beta$ 3 used in tracheal cartilage regeneration.

Overall, the PC@rhTGF nanofibrous scaffold with rhTGF- $\beta$ 3 is a good candidate for tracheal cartilage repair, due to its excellent physiochemical and biological properties. Structurally, the nanofibers could mimic the native structure of ECM to provide a suitable environment for WMSCs growth. Functionally, the released rhTGF- $\beta$ 3 could promote WMSCs chondrogenic differentiation. In addition, there are more superiorities using WMSCs in the cartilage regeneration than using other cells [44–46]. The WMSCs could be a promising seed cells in the construction of tissue-engineered tracheal cartilage.

#### 4. Conclusions

Core-shell nanofibrous scaffold encapsulated with rhTGF- $\beta$ 3 was fabricated by coaxial electrospinning in this study. The rhTGF- $\beta$ 3 released from PC@rhTGF nanofibrous scaffold in a sustained and stable manner for about 2 months. The bioactivity of rhTGF- $\beta$ 3 after releasing from the scaffold was well maintained during release process, and furthermore rhTGF- $\beta$ 3 could facilitate the synthesis of COL2 by chondrocytes. Most importantly, the PC@rhTGF nanofibrous scaffold enhanced the chondrogenic differentiation of WMSCs in vitro. PC@rhTGF nanofibrous scaffold fabricated in our study could serve as tissue engineered scaffold for tracheal cartilage regeneration.

#### Acknowledgements

This research was supported by National Natural Science Foundation of China (31370982, 31470941, 31271035), Ph.D. programs Foundation of Ministry of Education of China (20130075110005), Science and Technology Commission of Shanghai Municipality (15JC1490100, 15441905100), Yantai Double Hundred Talent Plan (20150812).

#### References

- [1] P.C. Cavadas, Tracheal reconstruction using a free Jejunal flap with cartilage skeleton: experimental study, *Plast. Reconstr. Surg.* 101 (1998) 937–942.
- [2] K. Kushibe, T. Tojo, H. Sakaguchi, M. Takahama, K. Nishizaki, K. Nezu, S. Taniguchi, Effects of warm ischemia and cryopreservation on cartilage viability of tracheal allografts, *Ann. Thorac. Surg.* 70 (2000) 1876–1879.
- [3] A. Messineo, R.M. Filler, T. Joseph, A. Bahoric, C.R. Smith, Tracheoplasty without stent, using preshaped cryopreserved cartilage allografts in neonatal pigs, *J. Pediatr. Surg.* 29 (1994) 697–700.
- [4] N. Okumura, T. NAKAMURA, Y. SHIMIZU, T. NATSUME, Y. IKADA, Experimental study of a new tracheal prosthesis made from collagen-grafted mesh, *ASAIO J.* 37 (1991) M317–M318.
- [5] H. Osada, K. Kojima, Experimental tracheal reconstruction with a rotated right stem bronchus, *Ann. Thorac. Surg.* 70 (2000) 1886–1890.
- [6] P. Macchiarini, P. Jungebluth, T. Go, M.A. Asnaghi, L.E. Rees, T.A. Cogan, A. Dodson, J. Martorell, S. Bellini, P.P. Parnigotto, Clinical transplantation of a tissue-engineered airway, *Lancet* 372 (2008) 2023–2030.
- [7] A. Gonfotti, M.O. Jaus, D. Barale, S. Baiguera, C. Comin, F. Lavorini, G. Fontana, O. Sibila, G. Rombolà, P. Jungebluth, The first tissue-engineered airway transplantation: 5-year follow-up results, *Lancet* 383 (2014) 238–244.
- [8] M. Berg, H. Ejnell, A. Kovács, N. Nayakawde, P.B. Patil, M. Joshi, L. Aziz, G. Rådberg, S. Hajizadeh, M. Olausson, Replacement of a tracheal stenosis with a tissue-engineered human trachea using autologous stem cells: a case report, *Tissue Eng. A* 20 (2013) 389–397.
- [9] C.A. Vacanti, K.T. Paige, W.S. Kim, J. Sakata, J. Upton, J.P. Vacanti, Experimental tracheal replacement using tissue-engineered cartilage, *J. Pediatr. Surg.* 29 (1994) 201–205.
- [10] D.Y. Kim, J. Pyun, J.W. Choi, J.H. Kim, J.S. Lee, H. Shin, H.J. Kim, H.N. Lee, B.H. Min, H.E. Cha, Tissue-engineered allograft tracheal cartilage using fibrin/hyaluronan composite gel and its in vivo implantation, *Laryngoscope* 120 (2010) 30–38.
- [11] N. Ketabchi, M. Naghibzadeh, M. Adabi, S.S. Esnaashari, R. Faridi-Majidi, Preparation and optimization of chitosan/polyethylene oxide nanofiber diameter using artificial neural networks, *Neural Comput. & Applic.* (2016) 1–13.
- [12] Z. Ma, C. Gao, Y. Gong, J. Shen, Cartilage tissue engineering PLLA scaffold with surface immobilized collagen and basic fibroblast growth factor, *Biomaterials* 26 (2005) 1253–1259.
- [13] F. Wiria, K. Leong, C. Chua, Y. Liu, Poly- $\epsilon$ -caprolactone/hydroxyapatite for tissue engineering scaffold fabrication via selective laser sintering, *Acta Biomater.* 3 (2007) 1–12.
- [14] X. Mo, C. Xu, M. Kotaki, S. Ramakrishna, Electrospun P (LLA-CL) nanofiber: a biomimetic extracellular matrix for smooth muscle cell and endothelial cell proliferation, *Biomaterials* 25 (2004) 1883–1890.
- [15] L. Tian, M.P. Prabhakaran, X. Ding, D. Kai, S. Ramakrishna, Emulsion electrospun vascular endothelial growth factor encapsulated poly(L-lactic acid-co- $\epsilon$ -caprolactone) nanofibers for sustained release in cardiac tissue engineering, *J. Mater. Sci.* 47 (2011) 3272–3281.
- [16] L. Tian, M.P. Prabhakaran, S. Ramakrishna, Strategies for regeneration of components of nervous system: scaffolds, cells and biomolecules, *Regen. Biomater.* 2 (2015) 31–45.
- [17] S. Hosseinzadeh, M. Mahmoudifard, F. Mohamadyar-Toupkanlou, M. Dodel, A. Hajarizadeh, M. Adabi, M. Soleimani, The nanofibrous PAN-PANI scaffold as an efficient substrate for skeletal muscle differentiation using satellite cells, *Bioprocess Biosyst. Eng.* (2016) 1–10.
- [18] L. Ma, C. Gao, J. Mao, J. Zhou, J. Shen, X. Hu, C. Han, Collagen/chitosan porous scaffolds with improved biostability for skin tissue engineering, *Biomaterials* 24 (2003) 4833–4841.
- [19] Z. Li, H.R. Ramay, K.D. Hauch, D. Xiao, M. Zhang, Chitosan–alginate hybrid scaffolds for bone tissue engineering, *Biomaterials* 26 (2005) 3919–3928.

- [20] T.A. Ahmed, E.V. Dare, M. Hincke, Fibrin: a versatile scaffold for tissue engineering applications, *Tissue Eng. B Rev.* 14 (2008) 199–215.
- [21] K. Kojima, C.A. Vacanti, Tissue engineering in the trachea, *Anat. Rec.* 297 (2014) 44–50.
- [22] S. Liu, K.D. Hou, M. Yuan, J. Peng, L. Zhang, X. Sui, B. Zhao, W. Xu, A. Wang, S. Lu, Q. Guo, Characteristics of mesenchymal stem cells derived from Wharton's jelly of human umbilical cord and for fabrication of non-scaffold tissue-engineered cartilage, *J. Biosci. Bioeng.* 117 (2014) 229–235.
- [23] H. Jiang, Y. Hu, Y. Li, P. Zhao, K. Zhu, W. Chen, A facile technique to prepare biodegradable coaxial electrospun nanofibers for controlled release of bioactive agents, *J. Control. Release* 108 (2005) 237–243.
- [24] L. Xiaoqiang, S. Yan, C. Rui, H. Chuanglong, W. Hongsheng, M. Xiumei, Fabrication and properties of core-shell structure P (LLA-CL) nanofibers by coaxial electrospinning, *J. Appl. Polym. Sci.* 111 (2009) 1564–1570.
- [25] F. Chen, P. Huang, X. Mo, Electrospinning of heparin encapsulated P (LLA-CL) core/shell nanofibers, *Nano Biomed. Eng.* 2 (2010) 84–90.
- [26] C. Vinatier, D. Mrugala, C. Jorgensen, J. Guicheux, D. Noël, Cartilage engineering: a crucial combination of cells, biomaterials and biofactors, *Trends Biotechnol.* 27 (2009) 307–314.
- [27] E. Grimaud, D. Heymann, F. Rédini, Recent advances in TGF- $\beta$  effects on chondrocyte metabolism: potential therapeutic roles of TGF- $\beta$  in cartilage disorders, *Cytokine Growth Factor Rev.* 13 (2002) 241–257.
- [28] M. Adabi, M. Naghibzadeh, M. Adabi, M.A. Zarrinfard, S.S. Esnaashari, A.M. Seifalian, R. Faridi-Majidi, H. Tanimowo Aiyelabegan, H. Ghanbari, Biocompatibility and nanostructured materials: applications in nanomedicine, *Artif. Cells Nanomed. Biotechnol.* (2016) 1–10.
- [29] C.R. Roberts, J.K. Rains, P.D. Paré, D.C. Walker, B. Wiggs, J.L. Bert, Ultrastructure and tensile properties of human tracheal cartilage, *J. Biomech.* 31 (1997) 81–86.
- [30] H. Seyednejad, W. Ji, F. Yang, C.F. van Nostrum, T. Vermonden, J.J. van den Beucken, W.J. Dhert, W.E. Hennink, J.A. Jansen, Coaxially electrospun scaffolds based on hydroxyl-functionalized poly ( $\epsilon$ -caprolactone) and loaded with VEGF for tissue engineering applications, *Biomacromolecules* 13 (2012) 3650–3660.
- [31] S. Yan, L. Xiaoqiang, T. Lianjiang, H. Chen, M. Xiumei, Poly (l-lactide-co- $\epsilon$ -caprolactone) electrospun nanofibers for encapsulating and sustained releasing proteins, *Polymer* 50 (2009) 4212–4219.
- [32] S. Sahoo, L.T. Ang, J.C.H. Goh, S.L. Toh, Growth factor delivery through electrospun nanofibers in scaffolds for tissue engineering applications, *J. Biomed. Mater. Res.* A 93 (2010) 1539–1550.
- [33] C.M. Valmikinathan, S. Defroda, X. Yu, Polycaprolactone and bovine serum albumin based nanofibers for controlled release of nerve growth factor, *Biomacromolecules* 10 (2009) 1084–1089.
- [34] Y. Zhang, X. Wang, Y. Feng, J. Li, C. Lim, S. Ramakrishna, Coaxial electrospinning of (fluorescein isothiocyanate-conjugated bovine serum albumin)-encapsulated poly ( $\epsilon$ -caprolactone) nanofibers for sustained release, *Biomacromolecules* 7 (2006) 1049–1057.
- [35] A. Jaklenec, A. Hinckfuss, B. Bilgen, D.M. Ciombor, R. Aaron, E. Mathiowitz, Sequential release of bioactive IGF-I and TGF- $\beta$  1 from PLGA microsphere-based scaffolds, *Biomaterials* 29 (2008) 1518–1525.
- [36] W. Ji, Y. Sun, F. Yang, J.J. van den Beucken, M. Fan, Z. Chen, J.A. Jansen, Bioactive electrospun scaffolds delivering growth factors and genes for tissue engineering applications, *Pharm. Res.* 28 (2011) 1259–1272.
- [37] Y. Su, Q. Su, W. Liu, M. Lim, J.R. Venugopal, X. Mo, S. Ramakrishna, S.S. Al-Deyab, M. El-Newehy, Controlled release of bone morphogenetic protein 2 and dexamethasone loaded in core-shell PLLACL-collagen fibers for use in bone tissue engineering, *Acta Biomater.* 8 (2012) 763–771.
- [38] C. Chung, J.A. Burdick, Engineering cartilage tissue, *Adv. Drug Deliv. Rev.* 60 (2008) 243–262.
- [39] S. Srouji, T. Kizhner, E. Suss-Tobi, E. Livne, E. Zussman, 3-D nanofibrous electrospun multilayered construct is an alternative ECM mimicking scaffold, *J. Mater. Sci. Mater. Med.* 19 (2008) 1249–1255.
- [40] C. Ribeiro, V. Sencadas, C. Caparrós, J. Ribelles, S. Lanceros-Méndez, Fabrication of poly(lactic acid)-poly(ethylene oxide) electrospun membranes with controlled micro to nanofiber sizes, *J. Nanosci. Nanotechnol.* 12 (2012) 6746–6753.
- [41] S. Peng, G. Jin, L. Li, K. Li, M. Srinivasan, S. Ramakrishna, J. Chen, Multi-functional electrospun nanofibres for advances in tissue regeneration, energy conversion & storage, and water treatment, *Chem. Soc. Rev.* 45 (2016) 1225–1241.
- [42] G. Jin, M.P. Prabhakaran, S. Ramakrishna, Stem cell differentiation to epidermal lineages on electrospun nanofibrous substrates for skin tissue engineering, *Acta Biomater.* 7 (2011) 3113–3122.
- [43] G. Jin, M.P. Prabhakaran, D. Kai, S. Ramakrishna, Controlled release of multiple epidermal induction factors through core-shell nanofibers for skin regeneration, *Eur. J. Pharm. Biopharm.* 85 (2013) 689–698.
- [44] R. Sarugaser, D. Lickorish, D. Baksh, M.M. Hosseini, J.E. Davies, Human umbilical cord perivascular (HUCPV) cells: a source of mesenchymal progenitors, *Stem Cells* 23 (2005) 220–229.
- [45] L. Wang, I. Tran, K. Seshareddy, M.L. Weiss, M.S. Detamore, A comparison of human bone marrow-derived mesenchymal stem cells and human umbilical cord-derived mesenchymal stromal cells for cartilage tissue engineering, *Tissue Eng. A* 15 (2009) 2259–2266.
- [46] M.L. Weiss, C. Anderson, S. Medicetty, K.B. Seshareddy, R.J. Weiss, I. VanderWerff, D. Troyer, K.R. McIntosh, Immune properties of human umbilical cord Wharton's jelly-derived cells, *Stem Cells* 26 (2008) 2865–2874.